Fast computation of the non-local boundary condition in Finite Difference Parabolic Equation radiowave propagation simulations

Christos Mias, *Member, IEEE*

***Abstract*—Finite Difference Parabolic Equation Method (FD-PEM) codes using a non-local boundary condition to model radiowave propagation over electrically large domains, require the computation of time consuming spatial convolution integrals. For the first time, we propose the use of recursive convolution (RC) with vector fitting to reduce this computational burden. RC is based on the ability to express functions as a sum of exponential terms. This is achieved using the vector fitting method. Details of the RC formulation applied in a two-dimensional (2D) Wide-Angle FD-PEM (WA-FD-PEM) are presented together with 2D simulations which demonstrate the computational speed and accuracy of the synthesized RC-WA-FD-PEM code.**

***Index Terms*— Finite-Difference Parabolic Equation Method, Recursive convolution, Vector Fitting, Radiowave propagation.**

I. Introduction

A computation time and memory efficient method for modelling electrically large radiowave propagation problems in which the effect of backward waves can be ignored is the Finite Difference Parabolic Equation Method (FD-PEM) [1-3]. The FD-PEM is suitable because it computes the forward propagating wave profile using a spatial marching process. This results in amenable computation time and memory requirements. It has been widely used by the wireless communications, broadcasting, optics, radar and computational electromagnetics communities in various electrically-large electromagnetic applications such as radiowave propagation modelling over rural and urban terrains [4], in radar cross-section simulations of airplanes, ships and other targets [5], in light guidance in various optical devices such as tapered waveguides and couplers [6] and X-ray diffraction [7].

Manuscript received September 24, 2007.

C. Mias is with the Applied Electromagnetics and High-Frequency Telecommunications Laboratory, Communications and Signal Processing Group, Electrical and Electronics Division, School of Engineering, University of Warwick, Coventry CV4 7AL, U.K.
(e-mail: christos.mias@warwick.ac.uk).

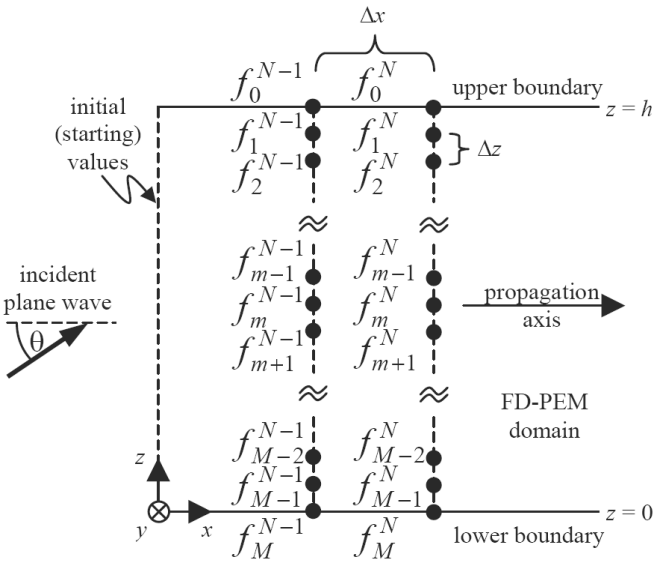

Fig.1. The Finite Difference Parabolic Equation Method (FD-PEM) marching scheme.

In the synthesis of FD-PEM software the boundary condition (BC) for truncating the computational domain is of particular interest. A variety of BC have been proposed such as the absorbing layer BC, the perfectly matched layer (PML) BC and the non-local BC [1].

The non-local BC [1, 8-10] is an exact BC that does not require the use of additional computation space in the form of absorbing layers. However, it has the disadvantage of the presence of a spatial convolution integral whose computation is time consuming. This computation is also memory demanding as it requires the storage and use of all previous values of the field along the boundary – hence the term "non-local BC". This paper demonstrates, for the first time, that recursive convolution (RC) with vector fitting can eliminate these disadvantages.

The RC has been employed for some time in power applications and circuit computations [11]. The RC relies on expressing the known term in the convolution integral as an exponential sum. Several methods can be used to achieve this. Here we use the vector fitting

method proposed by Gustavsen and Semlyen [12]. To demonstrate the use of RC in FD-PEM we focus, for simplicity, on 2D wide-angle FD-PEM (WA-FD-PEM) radiowave propagation simulations based on the Padé-(1,1) Claerbout approximation [1,2]. 2D PEM simulations have already been shown to produce useful results comparable to experimental measurements [13]. Furthermore, in the simulations shown, plane wave propagation is assumed at an angle and the FD-PEM computational domain is bounded by two non-local boundaries, an upper one and a lower one, as shown in Fig. 1.

In section II we present the 2D WA-FD-PEM formulation, the associated transmitting non-local boundary condition [10] and their finite difference discretisation. This is necessary mainly for completeness and because of the adoption of the exp(*jωt*) time harmonic variation, commonly used by electrical engineers. Section III shows the recursive convolution formulation and its finite difference implementation. Section IV deals with the application of the vector fitting method to obtain the exponential summation for the RC formulation. Section V demonstrates the accuracy and speed of the proposed RC-WA-FD-PEM method through plane wave simulations. Section VI concludes the paper.

II. The Wide Angle Parabolic Equation Method and its Finite Difference Discretisation

The Helmholtz equation describing the field distribution in our 2D homogeneous space, assumed here for simplicity to be free space is given by [14]

$$\frac{\partial^2 F(x,z)}{\partial x^2}+\frac{\partial^2 F(x,z)}{\partial z^2}+k_0^2 F(x,z)= \\ =\left(\frac{\partial}{\partial x}+jk_0\sqrt{1+q}\right)\left(\frac{\partial}{\partial x}-jk_0\sqrt{1+q}\right)F(x,z)=0 \tag{1}$$

$F(x,z)$ is the field variable, $F=E_y$ for TE polarization and $F=H_y$ for TM polarization. $k_0=2\pi/\lambda$ is the free space propagation constant and λ is the wavelength. The operator q is given by [14,15]

$$q=\frac{1}{k_0^2}\frac{\partial^2}{\partial z^2} \tag{2}$$

If we assume that the field variable has a time harmonic variation exp(*jωt*) and that we are interested only in the wave propagating in the positive *x*-direction, then we can neglect the operator bracket in (1) associated with the backward wave. Thus (1), as shown in [15], reduces to

$$\left(\frac{\partial}{\partial x}+jk_0\sqrt{1+q}\right)F(x,z)=0 \tag{3}$$

Let us now express the field variable as [15]

$$F(x,z)=f(x,z)\exp(-jk_0x) \tag{4}$$

where $f(x,z)$ is termed the reduced field variable and will be the variable used in the FD-PEM computations. Substituting (4) in (3) yields [15],

$$\frac{\partial f(x,z)}{\partial x}=-jk_0\left(\sqrt{1+q}-1\right)f(x,z) \tag{5}$$

Using the Padé-(1,1) Claerbout approximation [1,2]

$$\sqrt{1+q}\approx\frac{1+\frac{3}{4}q}{1+\frac{1}{4}q} \tag{6}$$

in (5), we have the following form amenable to finite difference discretisation

$$\left[1+\tfrac{1}{4}q\right]\frac{\partial f(x,z)}{\partial x}=-j\tfrac{1}{2}k_0qf(x,z) \tag{7}$$

It is interesting to note that substituting (2) in (7) leads to the differential equation

$$\frac{\partial^2 f(x,z)}{\partial z^2}-j2k_0\frac{\partial f(x,z)}{\partial x}-\frac{j}{2k_0}\frac{\partial^3 f(x,z)}{\partial z^2\partial x}=0 \tag{8}$$

that has the following solution

$$f(x,z)=A_0\exp\left(jk_0\frac{2\sin^2\theta}{4-\sin^2\theta}x\right)\exp\left(-jk_0\sin\theta\, z\right) \tag{9}$$

which, for fairly wide angles [2], is a good approximation to the reduced wave field plane wave solution of (1)

$$f(x,z)=A_0\exp\left[jk_0(1-\cos\theta)\,x\right]\exp\left(-jk_0\sin\theta\, z\right) \tag{10}$$

hence the name 'wide-angle' FD-PEM [14]. Equation (9) will be the incident wave to our WA-FD-PEM simulations. Both (9) and (10) have identical values at $x = 0$.

The transmitting non-local BC is defined [10] at the upper boundary ($z = h$) and the lower boundary ($z = 0$) as

$$\frac{\partial f(x,z)}{\partial z} = \frac{\partial f^{inc}(x,z)}{\partial z} - j\chi 2k_0 \int_0^x w(x-\xi)\frac{\partial f(\xi,z)}{\partial \xi} d\xi + \underbrace{j\chi 2k_0 \int_0^x w(x-\xi)\frac{\partial f^{inc}(\xi,z)}{\partial \xi} d\xi}_{y_{inc}(x)} \tag{11}$$

$$w(x) = J_0(k_0 x)\, e^{-jk_0 x} \tag{12}$$

where $\chi = 1$ for the upper boundary and $\chi = -1$ for the lower boundary. $f^{inc}(x,z)$ is the incident field which should be known everywhere along the boundary. For simplicity, in this paper we assume it is defined by (9). $J_\nu(r)$ is the Bessel function of the first kind and ν order.

Based on the nomenclature of Fig. 1, the reduced field variable and its derivatives in (7) or (8) are discretised as follows using the central difference approximation [1]

$$f[(N-\tfrac{1}{2})\Delta x,(M-m)\Delta z] \approx \frac{f_m^N + f_m^{N-1}}{\Delta x} \tag{13}$$

$$\frac{\partial f[(N-\tfrac{1}{2})\Delta x,(M-m)\Delta z]}{\partial x} \approx \frac{f_m^N - f_m^{N-1}}{\Delta x} \tag{14}$$

$$\frac{\partial^2 f[N\Delta x,(M-m)\Delta z]}{\partial z^2} \approx \frac{f_{m-1}^N - 2f_m^N + f_{m+1}^N}{(\Delta z)^2} \tag{15}$$

Substituting (13)-(15) in (7) or (8) yields

$$\alpha_N f_{m-1}^N + \beta_N f_m^N + \alpha_N f_{m+1}^N = \alpha_{N-1} f_{m-1}^{N-1} + \beta_{N-1} f_m^{N-1} + \alpha_{N-1} f_{m+1}^{N-1} \tag{16}$$

where

$$\alpha_N = \frac{\frac{1}{k_0} + j\Delta x}{4k_0(\Delta z)^2}, \quad \alpha_{N-1} = \frac{\frac{1}{k_0} - j\Delta x}{4k_0(\Delta z)^2} \tag{17}$$

$$\beta_N = 1 - \frac{\frac{1}{k_0} + j\Delta x}{2k_0(\Delta z)^2}, \quad \beta_{N-1} = 1 - \frac{\frac{1}{k_0} - j\Delta x}{2k_0(\Delta z)^2} \tag{18}$$

At the two boundaries we will employ the 2nd order accurate discretisation of the derivative $\partial f / \partial z$ described in [14]. Thus, at the upper and lower boundaries

$$\frac{\partial f(N\Delta x,h)}{\partial z} \approx \frac{3f_0^N - 4f_1^N + f_2^N}{2\Delta z} \tag{19}$$

$$\frac{\partial f(N\Delta x,0)}{\partial z} \approx -\frac{3f_M^N - 4f_{M-1}^N + f_{M-2}^N}{2\Delta z} \tag{20}$$

Furthermore, the integral terms in (11) can be expressed as follows [10]

$$j\chi 2k_0 \int_0^x w(x-\xi)\frac{\partial g(\xi,z)}{\partial \xi} d\xi = j\chi 2k_0 \int_0^{N\Delta x} w(N\Delta x-\xi)\frac{\partial g(\xi,z)}{\partial \xi} d\xi \tag{21}$$

$$\approx \chi a_N g_A^N - \sum_{n=0}^{N-1} \chi b_n g_A^n$$

$$a_N = \frac{2j}{\Delta x} Q(k_0 \Delta x) \tag{22}$$

$$b_0 = \frac{2j}{\Delta x}\{Q(k_0 N\Delta x) - Q[k_0(N-1)\Delta x]\} \tag{23}$$

$$b_n = \frac{2j}{\Delta x}\{-Q[k_0(N-n+1)\Delta x] + 2Q[k_0(N-n)\Delta x] - Q[k_0(N-n-1)\Delta x]\} \quad \text{for } n>0 \tag{24}$$

$$Q(r) = r\, e^{-jr}\left[J_0(r) + jJ_1(r)\right] \tag{25}$$

where at the upper boundary $A = 0$ and at the lower boundary $A = M$. For the first integral term in (11) $g = f$ and for the second one $g = f^{inc}$. From (11), (19), (20) and (21) it follows that

$$f_A^N = \rho f_B^N + \eta f_C^N + \Xi_{N,A} \tag{26}$$

where at the upper boundary $A = 0$, $B = 1$, $C = 2$ and at the lower boundary $A = M$, $B = M-1$ and $C = M-2$. In addition,

$$\rho = 4/(3 + 2a_N \Delta z) \tag{27}$$

$$\eta = -1/(3 + 2a_N \Delta z) \tag{28}$$

$$\Xi_{N,A} = f_A^{inc,N} - \rho f_B^{inc,N} - \eta f_C^{inc,N} + \frac{\rho \Delta z}{2} \sum_{n=0}^{N-1} b_n \left(f_A^n - f_A^{inc,n}\right) \tag{29}$$

From (16) and the boundary condition (26), the following global matrix equation is assembled to solve the problem in Fig. 1,

$$\mathbf{\Lambda_N F_N} = \mathbf{\Lambda_{N-1} F_{N-1}} + \mathbf{\Omega} \tag{30}$$

where details of the matrices/vectors are given in the Appendix.

III. Recursive Convolution and its Implementation

If the function w in the convolution term in (21) can be expressed as $A_i \exp(B_i x)$ then

$$\begin{aligned} R(x) &= \int_0^x w(x-\xi)\frac{\partial g(\xi,z)}{\partial \xi}d\xi \\ &= R_i(x) = \int_0^x A_i e^{B_i(x-\xi)}\frac{\partial g(\xi,z)}{\partial \xi}d\xi \\ &= R_i(N\Delta x) = \int_0^{N\Delta x} A_i e^{B_i(N\Delta x-\xi)}\frac{\partial g(\xi,z)}{\partial \xi}d\xi \\ &= R_i^N \end{aligned} \tag{31}$$

Therefore

$$\begin{aligned} R_i^{N-1} &= R_i[(N-1)\Delta x] \\ &= \int_0^{(N-1)\Delta x} A_i e^{B_i[(N-1)\Delta x-\xi]}\frac{\partial g(\xi,z)}{\partial \xi}d\xi \end{aligned} \tag{32}$$

From (31) and (32) the following recursive formula can be derived

$$R_i^N = e^{B_i\Delta x}R_i^{N-1} + \int_{(N-1)\Delta x}^{N\Delta x} A_i e^{B_i(N\Delta x-\xi)}\frac{\partial g(\xi,z)}{\partial \xi}d\xi \tag{33}$$

In general $w(x)$ is approximately expressed as

$$w(x) \approx \tilde{w}(x) = \sum_{i=1}^{T} A_i e^{B_i x} \tag{34}$$

thus

$$\begin{aligned} R(x) = R^N &\approx \sum_{i=1}^{T} R_i(x) = \sum_{i=1}^{T} R_i^N = \sum_{i=1}^{T} e^{B_i\Delta x}R_i^{N-1} \\ &+ \sum_{i=1}^{T} A_i e^{B_i N\Delta x}\int_{(N-1)\Delta x}^{N\Delta x} e^{-B_i\xi}\frac{\partial g(\xi,z)}{\partial \xi}d\xi \end{aligned} \tag{35}$$

where $R_i^0 = 0$. It is seen from the RC formulation (35) that only the T convolution values, R_i^{N-1} at the previous step *N-1*, need to be stored in computer memory whereas the standard convolution requires the memory storage of all the previous field values.

The integral term in (35) can be discretised as follows

$$\begin{aligned} &\int_{(N-1)\Delta x}^{N\Delta x} e^{-B_i\xi}\frac{\partial g(\xi,z)}{\partial \xi}d\xi \\ &\approx \int_{(N-1)\Delta x}^{N\Delta x} e^{-B_i\xi}\frac{g(N\Delta x,z)-g[(N-1)\Delta x,z]}{\Delta x}d\xi \\ &= \left\{\frac{g(N\Delta x,z)}{\Delta x} - \frac{g[(N-1)\Delta x,z]}{\Delta x}\right\}\int_{(N-1)\Delta x}^{N\Delta x} e^{-B_i\xi}d\xi \\ &= e^{-B_i N\Delta x}\left\{\frac{g(N\Delta x,z)}{\Delta x} - \frac{g[(N-1)\Delta x,z]}{\Delta x}\right\}\left(\frac{1-e^{B_i\Delta x}}{-B_i}\right) \end{aligned} \tag{36}$$

From (35) and (36) it follows that

$$\begin{aligned} &j\chi 2k_0\int_0^x w(x-\xi)\frac{\partial g(\xi,z)}{\partial \xi}d\xi \\ &\qquad \approx \tau\chi g_A^N - \tau\chi g_A^N + \chi\Psi_{N,A}^g \end{aligned} \tag{37}$$

$$\tau = 2jk_0\sum_{i=1}^{T} A_i\left(\frac{1-e^{B_i\Delta x}}{-B_i\Delta x}\right) \tag{38}$$

$$\Psi_{N,A}^g = 2jk_0\sum_{i=1}^{T} e^{B_i\Delta x}R_i^{N-1} \tag{39}$$

Generally there are different values of R_i at the upper and lower boundaries.

From (11), using (19), (20) and (37), we obtain an expression identical in form to (26) where now ρ, η, and $\Xi_{N,A}$ are

$$\rho = 4/(3+2\tau\Delta z) \tag{40}$$

$$\eta = -1/(3+2\tau\Delta z) \tag{41}$$

$$\begin{aligned} \Xi_{N,A} &= f_A^{inc,N} - \rho f_B^{inc,N} - \eta f_C^{inc,N} \\ &+ \frac{\rho\tau\Delta z}{2}\left(f_A^{N-1} - f_A^{inc,N-1}\right) - \frac{\rho\Delta z}{2}\left(\Psi_{N,A} - \Psi_{N,A}^{inc}\right) \end{aligned} \tag{42}$$

where $\Psi_{N,A} = \Psi_{N,A}^g$ for $g = f$ and $\Psi_{N,A}^{inc} = \Psi_{N,A}^g$ for $g = f^{inc}$.

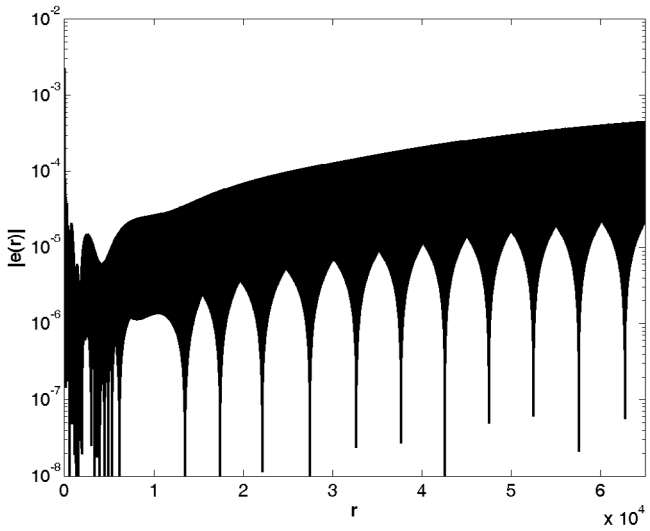

Fig.2. Absolute value of the vector fitting error, $|e(r)|$.

IV. The Vector Fitting approximation

As indicated in (34) the function $w(x)$ must be curve fitted with a function $\widetilde{w}(x)$ which is a summation of exponential terms, $A_i \exp(B_i x)$, where A_i and B_i are complex numbers. To achieve this we use first the vector fitting (VF) method [12] to express the function $u(r) = J_0(r)$ as a sum of exponential terms. In the VF method, the Laplace transform, $U(s)$, of $u(r)$ is approximated with a sum of fractions $a_i/(s-b_i)$, i.e.

$$U(s) = \frac{1}{\sqrt{s^2+1}} \approx \sum_{i=1}^{T} \frac{c_i}{s-d_i} \tag{43}$$

thus

$$u(r) = J_0(r) \approx \widetilde{u}(r) = \sum_{i=1}^{T} c_i e^{d_i r} \tag{44}$$

$u(r)$ is curve fitted over the argument region $0 \le r \le 65000$. We have found that $T = 20$ is sufficient for our computations. The (c_i, d_i) values are listed in Table I for reference. The table also contains input parameters to the VECTFIT software [12] which is available in the public domain. Fig. 2 shows that the absolute value of the vector fitting error defined as $|e(r)| \equiv |\widetilde{u}(r) - u(r)|$. From (12)

$$w(x) = J_0(k_0 x)\, e^{-jk_0 x} \approx \sum_{i=1}^{T} c_i e^{d_i k_0 x} e^{-jk_0 x} \tag{45}$$

From (34) and (45) it follows that $A_i = c_i$ and $B_i = k_0(d_i - j)$.

TABLE I
Coefficients of the Exponential Terms

i	c_i
1	$1.200089153095126\times10^{-1} - j\ 8.887110272709117\times10^{-2}$
2	$1.200089153095126\times10^{-1} + j\ 8.887110272709117\times10^{-2}$
3	$5.978377598686671\times10^{-2} - j\ 5.319444730272732\times10^{-2}$
4	$5.978377598686671\times10^{-2} + j\ 5.319444730272732\times10^{-2}$
5	$2.496343795730085\times10^{-1} - j\ 8.352042401788233\times10^{-2}$
6	$2.496343795730085\times10^{-1} + j\ 8.352042401788233\times10^{-2}$
7	$3.134548793789095\times10^{-2} - j\ 2.962271240527257\times10^{-2}$
8	$3.134548793789095\times10^{-2} + j\ 2.962271240527257\times10^{-2}$
9	$1.688437967823251\times10^{-2} - j\ 1.635817566058171\times10^{-2}$
10	$1.688437967823251\times10^{-2} + j\ 1.635817566058171\times10^{-2}$
11	$9.266101367312587\times10^{-3} - j\ 9.096008962608301\times10^{-3}$
12	$9.266101367312587\times10^{-3} + j\ 9.096008962608301\times10^{-3}$
13	$5.190856055158444\times10^{-3} - j\ 5.145786812716612\times10^{-3}$
14	$5.190856055158444\times10^{-3} + j\ 5.145786812716612\times10^{-3}$
15	$3.059157825293548\times10^{-3} - j\ 3.074949610893679\times10^{-3}$
16	$3.059157825293548\times10^{-3} + j\ 3.074949610893679\times10^{-3}$
17	$2.133795019701758\times10^{-3} - j\ 2.282877026283986\times10^{-3}$
18	$2.133795019701758\times10^{-3} + j\ 2.282877026283986\times10^{-3}$
19	$1.566230572725720\times10^{-3} - j\ 1.325831207539377\times10^{-3}$
20	$1.566230572725720\times10^{-3} + j\ 1.325831207539377\times10^{-3}$
i	d_i
1	$-2.862025157924029\times10^{-1} + j\ 9.513814754101411\times10^{-1}$
2	$-2.862025157924029\times10^{-1} - j\ 9.513814754101411\times10^{-1}$
3	$-8.611173459526850\times10^{-2} + j\ 9.940793355694457\times10^{-1}$
4	$-8.611173459526850\times10^{-2} - j\ 9.940793355694457\times10^{-1}$
5	$-8.180577336750963\times10^{-1} + j\ 5.723494136898141\times10^{-1}$
6	$-8.180577336750963\times10^{-1} - j\ 5.723494136898141\times10^{-1}$
7	$-2.605016991017936\times10^{-2} + j\ 9.991234242291304\times10^{-1}$
8	$-2.605016991017936\times10^{-2} - j\ 9.991234242291304\times10^{-1}$
9	$-8.045953130594308\times10^{-3} + j\ 9.998466286667713\times10^{-1}$
10	$-8.045953130594308\times10^{-3} - j\ 9.998466286667713\times10^{-1}$
11	$-2.537081506691435\times10^{-3} + j\ 9.999687922562992\times10^{-1}$
12	$-2.537081506691435\times10^{-3} - j\ 9.999687922562992\times10^{-1}$
13	$-8.109994368351026\times10^{-4} + j\ 9.999916154004553\times10^{-1}$
14	$-8.109994368351026\times10^{-4} - j\ 9.999916154004553\times10^{-1}$
15	$-2.535265393448782\times10^{-4} + j\ 9.999960071583445\times10^{-1}$
16	$-2.535265393448782\times10^{-4} - j\ 9.999960071583445\times10^{-1}$
17	$-6.283786018711213\times10^{-5} + j\ 9.999964647482276\times10^{-1}$
18	$-6.283786018711213\times10^{-5} - j\ 9.999964647482276\times10^{-1}$
19	$-2.692908742302214\times10^{-6} + j\ 9.999980044508565\times10^{-1}$
20	$-2.692908742302214\times10^{-6} - j\ 9.999980044508565\times10^{-1}$

VECTFIT input parameters: (a) 30000 frequency samples; (b) angular frequency range $0 \le \omega \le \pi$; (c) $T = 20$; (d) the number of iterations is 10. These coefficients are generic i.e. they are valid for different frequencies, different discretisation steps and different geometric 2D models.

TABLE II
SIMULATION TIMES FOR CONVOLUTION INTEGRAL (IN SECONDS)*

Computation Method	Number of Steps			
	1000	2000	3000	100000
trapezoidal integration	79.1	312.3	708.5	–
Dalrymple and Martin [10]	378.9	1540.0	3406.2	–
RC	1.5	2.2	3.0	291.0

*MATLAB CPU time.
$z = 2$ m

V. NUMERICAL RESULTS

The computations were made on a PC (Intel Pentium 4 CPU, 3.2 GHz). The simulation parameters are $\theta = 25°$, $\lambda = 0.1$ m, $\Delta x = 0.01$ m, $\Delta z = 0.01$ m $h = 2$ m, $A_0 = 1$ (refer to Fig. 1 and (9)).

A. Investigation of Recursive Convolution Formulation

The recursive convolution (RC) formulation is first investigated before its FD-PEM implementation. To do this we consider the second convolution term in (11), $y_{inc}(x)$, which is in terms of the known incident field (9). We employ the RC formulation (37). The RC result is compared with the formulation of [10] as described by (21). The computations are done in MATLAB. Results are also presented from the application of trapezoidal integration (using the 'trapz' MATLAB command) to compute the integral term $y_{inc}(x)$. In the latter method the derivative term $\partial f^{inc}/\partial \xi$ is expressed analytically. The real and imaginary parts of the convolution term $y_{inc}(x)$ are shown in Fig. 3. The results confirm that the RC methodology, the VF exponential sum and the approach followed for the discretisation of the derivative term $\partial f^{inc}/\partial \xi$ are acceptable. The computation time for each of the methods is shown in Table II. As the number of steps increases the computation times for the trapezoidal integration method and the Dalrymple and Martin method increase significantly. Hence, for these methods, time data are not shown for 100000 steps. This number of steps corresponds to a distance $x = 1$ km which is a practical distance for a hypothetical wireless system operating at 3 GHz. In contrast, the RC formulation is very fast.

B. Free space plane wave propagation

The RC-WA-FD-PEM is used to model plane wave propagation at an angle $\theta = 25°$ to the preferred axis of propagation (the x-axis) as shown in Fig. 1. This example was chosen because it has both an upper and a lower non-local boundary, it has an exact analytic solution and inaccuracies due to the angular limitations of the Claerbout approximation are avoided as we can control the maximum angle of wave propagation.

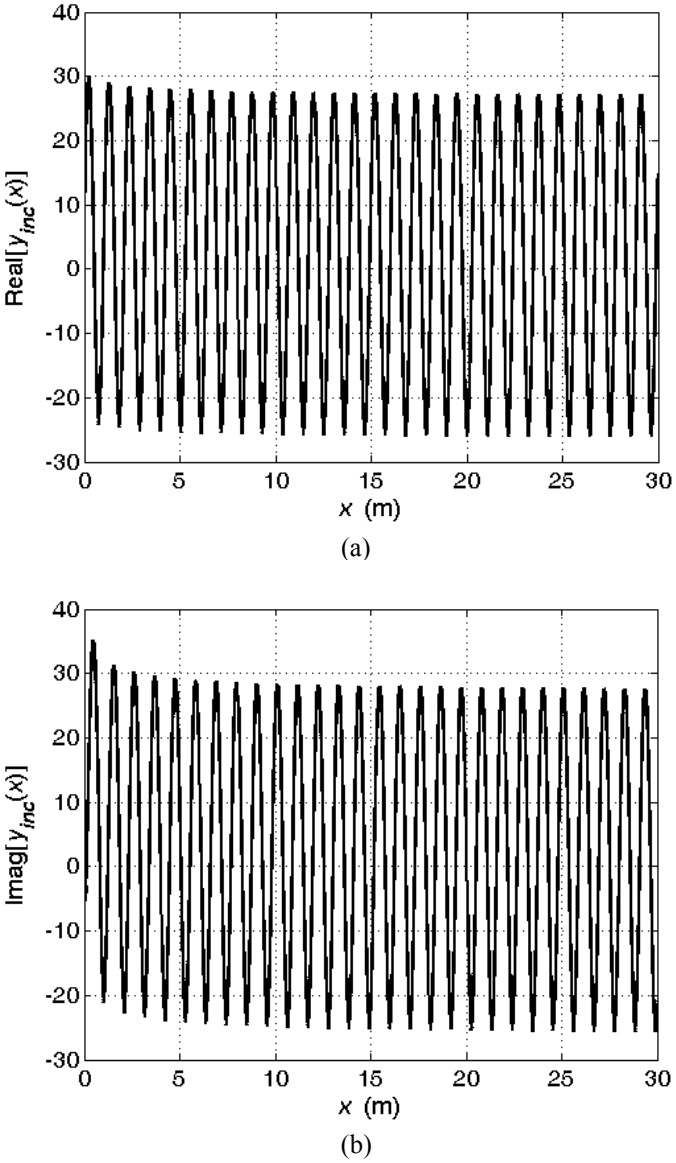

Fig.3. Plot of (a) the real part and (b) the imaginary part of $y_{inc}(x)$ in (11). Dashed line: trapezoidal integration; dotted line: Dalrymple and Martin [10]; solid line: RC. The three curves are superimposed. As the three methodologies are not identical, a small difference between the curves is expected. The difference in value between the trapezoidal integration and one of the other two methods falls between the bounds ±0.65 for both the real and imaginary parts. The difference in value between the Dalrymple and Martin and the RC method falls between the bounds ±0.02 for both the real and imaginary parts.

The wave at the starting plane ($x = 0$) is the plane wave solution to the parabolic equation (9).

To numerically demonstrate the speed, stability and accuracy of the RC-WA-FD-PEM code, simulations are presented over a propagation range of 10000 steps ($x = 100$ m) and 100000 steps ($x = 1$ km). Both axial and transverse results are presented. The results are compared with the analytical results obtained from (9) and with results obtained using the "standard convolution" WA-FD-PEM approach of Dalrymple and

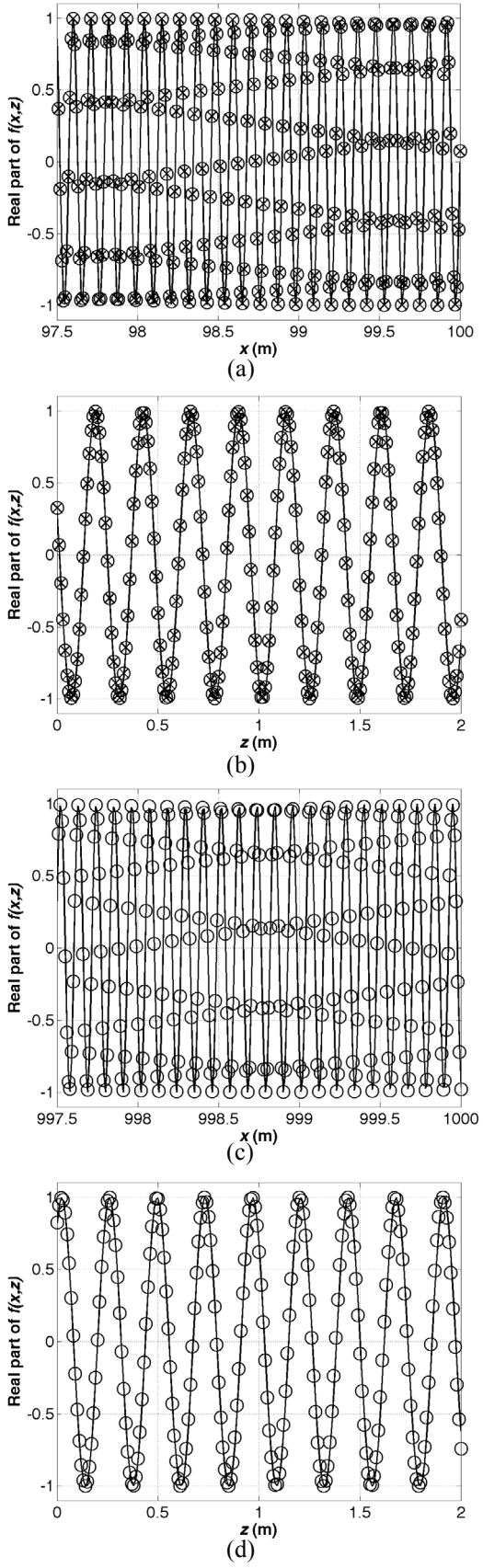

Fig.4. (a,b) 10000 steps; (c,d) 100000 steps. (a) z = 1 m; (b) x = 95 m; (c) z = 1 m; (d) x = 995 m.
○: RC-WA-FD-PEM; ×: Dalrymple and Martin [10] WA-FD-PEM; solid line: analytic solution.

TABLE III
SIMULATION TIMES FOR WA-FD-PEM METHODS (IN SECONDS)*

WA-FD-PEM Method	Number of Steps	
	10000	100000
WA-FD-PEM Dalrymple & Martin [10]	1344.6	–
RC-WA-FD-PEM	3.9	34.5

*Real time. FORTRAN 77 codes. Codes were run through MATLAB.

Martin [10]. Again, for the latter method, no results are shown for the 100000-step model due to the large computation time required.

The 10000-step results in Fig. 4a,b confirm that the RC-WA-FD-PEM is as accurate as the Dalrymple and Martin WA-FD-PEM. Furthermore, the results of both methods agree very well with the analytical results. In addition, Fig. 4c,d show that the RC-WA-FD-PEM results do not show any instability or deterioration in accuracy for the larger range of 100000 steps. Table III confirms the remarkable speed advantage of the RC-WA-FD-PEM.

VI. CONCLUSION

A novel RC-WA-FD-PEM methodology has been proposed for 2D radiowave propagation simulations. All our numerical results suggest that the method is fast, accurate and stable.

It must be noted that in many parabolic equation method simulations involving complicated environments in which the source field at the starting plane is confined within the computational domain and it is thus zero at the boundary, there is no need to use the transmitting non-local boundary condition employed in this paper. For example, if the boundary lies in free space as in the paper, it is sufficient to use the simpler diffractive non-local boundary condition [1]. The latter boundary condition does not include the incident field terms in (11). Hence since the proposed methodology is applicable to the transmitting non-local boundary condition then it is also applicable to the corresponding simpler diffractive non-local boundary condition.

Current research focuses on the application of the proposed recursive convolution methodology to the very-wide-angle FD-PEM proposed in [16] and to 3D PEM [1]. In addition, it will be informative to compare the computational requirements of the proposed RC-WA-FD-PEM with those of a WA-FD-PEM incorporating a local boundary condition such as a PML.

APPENDIX

Details of the matrices/vectors of the global matrix equation (30):

$$\mathbf{\Lambda_N} = \begin{bmatrix} \beta'_N & \alpha'_N & 0 & \cdots & 0 & 0 & 0 \\ \alpha_N & \beta_N & \alpha_N & \cdots & 0 & 0 & 0 \\ 0 & \alpha_N & \beta_N & \cdots & 0 & 0 & 0 \\ \vdots & \vdots & \vdots & \vdots & \vdots & \vdots & \vdots \\ 0 & 0 & 0 & \cdots & \beta_N & \alpha_N & 0 \\ 0 & 0 & 0 & \cdots & \alpha_N & \beta_N & \alpha_N \\ 0 & 0 & 0 & \cdots & 0 & \alpha'_N & \beta'_N \end{bmatrix} \tag{A1}$$

where $\beta'_N = \beta_N + \alpha_N \rho \qquad \alpha'_N = \alpha_N + \alpha_N \eta$.

$$\mathbf{\Lambda_{N-1}} = \begin{bmatrix} \beta_{N-1} & \alpha_{N-1} & 0 & \cdots & 0 & 0 & 0 \\ \alpha_{N-1} & \beta_{N-1} & \alpha_{N-1} & \cdots & 0 & 0 & 0 \\ 0 & \alpha_{N-1} & \beta_{N-1} & \cdots & 0 & 0 & 0 \\ \vdots & \vdots & \vdots & \vdots & \vdots & \vdots & \vdots \\ 0 & 0 & 0 & \cdots & \beta_{N-1} & \alpha_{N-1} & 0 \\ 0 & 0 & 0 & \cdots & \alpha_{N-1} & \beta_{N-1} & \alpha_{N-1} \\ 0 & 0 & 0 & \cdots & 0 & \alpha_{N-1} & \beta_{N-1} \end{bmatrix} \tag{A2}$$

$$\mathbf{F_N} = \begin{bmatrix} f_1^N \\ f_2^N \\ f_3^N \\ \vdots \\ f_{M-3}^N \\ f_{M-2}^N \\ f_{M-1}^N \end{bmatrix} \mathbf{F_{N-1}} = \begin{bmatrix} f_1^{N-1} \\ f_2^{N-1} \\ f_3^{N-1} \\ \vdots \\ f_{M-3}^{N-1} \\ f_{M-2}^{N-1} \\ f_{M-1}^{N-1} \end{bmatrix} \mathbf{\Omega} = \begin{bmatrix} \alpha_{N-1} f_0^{N-1} \\ 0 \\ 0 \\ \vdots \\ 0 \\ 0 \\ \alpha_{N-1} f_M^{N-1} \end{bmatrix} - \begin{bmatrix} \alpha_N \Xi_{N,0} \\ 0 \\ 0 \\ \vdots \\ 0 \\ 0 \\ \alpha_N \Xi_{N,M} \end{bmatrix} \tag{A3}$$

REFERENCES

[1] M. Levy, *Parabolic equation methods for electromagnetic wave propagation*, The IEE (The Institute of Electrical Engineers), 2000.

[2] D. Lee and S.T. McDaniel, "Ocean acoustic propagation by finite difference methods", *J. Comp. & Math. with Appl.*, vol. 24, pp. 305-423, 1987.

[3] F.B. Jensen, W.A. Kuperman, M.B. Porter, H. Schmidt, *Computational Ocean Acoustics*, AIP (American Intitute of Physics) Press, 1994.

[4] M.F. Levy, "Parabolic equation modelling of propagation over irregular terrain", *Electronics Letters*, vol. 26, no. 15, pp. 1153-1155, 1990.

[5] M.F. Levy and P.-P. Borsboom, "Radar cross-section computations using the parabolic equation method", *Electronics Letters*, vol. 32, no. 13, pp.1234-1236, 1996.

[6] R. Scarmozzino and R.M. Osgood, Jr., "Comparison of finite-difference and Fourier transform solutions of the parabolic wave equation with emphasis on integrated-optics applications", *Journal of Optical Society of America*, vol. 8, no. 5, pp. 724-731, 1991.

[7] Y.V. Kopylov, A.V. Popov, A.V. Vinogradov, "Application of the parabolic equation to X-ray diffraction optics, *Optics Communications*, vol. 118, pp. 619-636, 1995.

[8] S.W. Marcus, "A hybrid (finite difference – surface Green's function) method for computing transmission losses in an inhomogeneous atmosphere over irregular terrain", *IEEE Transactions on Antennas and Propagation*, vol. 40, no. 12, pp. 1451-1458, 1992.

[9] A. V. Popov, "Transparent boundaries for the parabolic wave equation", *Journal of Mathematical Sciences*, vol. 96, no. 4, pp. 3415-3418, 1999.

[10] Dalrymple, R. A. and P. A. Martin, "Perfect boundary conditions for parabolic water-wave models," *Proc. R. Soc. London A*, vol. 437, pp. 41–54, 1992.

[11] A. Semlyen and A. Dabuleanu, "Fast and accurate switching transient calculations on transmission lines with ground return using recursive convolutions," *IEEE Trans. Power App. Syst.*, vol. PAS-94, no. 2, pp. 561–571, 1975.

[12] B. Gustavsen, and A. Semlyen, "Rational Approximation of Frequency Domain Responses by Vector Fitting", *IEEE Trans. on Power Delivery*, vol. 14, no. 3, pp. 1052-1061, 1999.

[13] N. Geng and W. Wiesbeck, "Parabolic equation method simulations compared to measurements", IEE Antennas and Propagation Conference, 4-7 April 1995, IEE Conference Publication No. 407, pp. 359-362.

[14] M. West, K. Gilbert and R.A. Sack, "A tutorial on the Parabolic equation (PE) model used for long range sound propagation in the atmosphere", *Applied Acoustics*, vol. 37, pp. 31-49, 1992.

[15] C. Mias and C.C. Constantinou, "Modelling of plane wave transmission through a periodic array of cylinders with the Parabolic Equation Method". *Microwave and Optical Technology Letters*, vol. 19, no. 1, pp. 78-84, 1998.

[16] A. Zebic-Le Hyaric, "Wide-Angle Nonlocal Boundary Conditions for the Parabolic Wave Equation*", IEEE Transactions on Antennas and Propagation*, vol. 49, no. 6, pp. 916–922, 2001.